

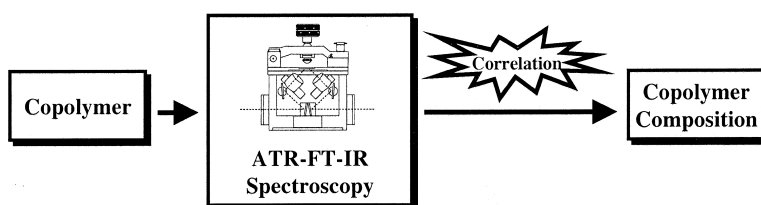
Article

High-Throughput Evaluation of Olefin Copolymer Composition by Means of Attenuated Total Reflection Fourier Transform Infrared Spectroscopy

Arno Tuchbreiter, Jrgen Marquardt, Jrg Zimmermann, Philipp Walter, Rolf Mlhaupt, Bernd Kappler, Daniel Faller, Tobias Roths, and Josef Honerkamp

J. Comb. Chem., **2001**, 3 (6), 598-603 • DOI: 10.1021/cc010033q • Publication Date (Web): 24 October 2001

Downloaded from <http://pubs.acs.org> on March 20, 2009



More About This Article

Additional resources and features associated with this article are available within the HTML version:

- Supporting Information
- Access to high resolution figures
- Links to articles and content related to this article
- Copyright permission to reproduce figures and/or text from this article

[View the Full Text HTML](#)

High-Throughput Evaluation of Olefin Copolymer Composition by Means of Attenuated Total Reflection Fourier Transform Infrared Spectroscopy

Arno Tuchbreiter,* Jürgen Marquardt, Jörg Zimmermann, Philipp Walter, and Rolf Mülhaupt

Freiburger Materialforschungszentrum und Institut für Makromolekulare Chemie der Albert-Ludwigs Universität Freiburg, Stefan-Meier-Strasse 21, D-79104 Freiburg, Germany

Bernd Kappler, Daniel Faller, Tobias Roths, and Josef Honerkamp

Fakultät für Physik, Albert-Ludwigs Universität Freiburg, Hermann-Herder-Strasse 3, D-79104 Freiburg, Germany

Received June 4, 2001

As a consequence of developing fully automated reactors for organic and organometallic synthesis and polymerizations combined with rapid on-line analysis, databases, and data mining, the analysis of polymers with respect to composition and properties has been speeded up. High-throughput evaluation of olefin copolymers requires fast measurements and high accuracy without tedious sample preparation such as pressing KBr pellets. This has been achieved by using attenuated total reflection Fourier transform infrared spectroscopy (ATR-FTIR spectroscopy) in conjunction with multivariate calibration in order to determine the composition of olefin copolymers such as ethene/propene, ethene/1-hexene and ethene/1-octene copolymers.

Introduction

Over the past 10 years, the number of applications of new synthesis techniques called “high-throughput screening” or “combinatorial chemistry” has increased dramatically.¹ This new research technology has been first adopted by the pharmaceutical industry to accelerate proceedings in drug discovery by means of creating large libraries and then testing them for activity. Since then, the new technology has expanded to other industries producing catalysts, polymers, and advanced materials. Over the past 5 years companies have developed a large number of now reliable laboratory robotic systems for high-speed chemistry evaluation.² High-throughput evaluation is becoming cost effective because a large number of experiments require much less time and resources. More than ever, new rapid screening techniques are required to analyze the large amounts of synthesized products for the development of new materials.³ Here, we report on a rapid novel technique based on attenuated total reflection Fourier transform infrared spectroscopy (ATR-FTIR spectroscopy), which provides a powerful tool for determining the composition of olefin copolymers such as ethene/propene, ethene/1-hexene, and ethene/1-octene copolymers. Conventional polymer characterization by ¹³C NMR spectroscopy⁴ is both cost- and time-intensive. A significant acceleration of analyses can be achieved by using FTIR spectroscopy.⁵ Unfortunately, traditional FTIR still requires time-consuming sample preparation, e.g., for compression molding of KBr pellets. In sharp contrast, ATR-FTIR spectroscopy allows the direct characterization of

powders and solid polymers without any further preprocessing and thus meets the demands of high-throughput evaluation of transition metal catalyzed olefin polymerization.

ATR-FTIR Spectroscopy

The original single-reflection experimental setup of ATR spectroscopy was established by Harrick⁶ and Fahrenfort,⁷ who described quantitatively the differences between transmission and ATR spectra. When light is passing through two media from one having a larger refraction index (crystal) with an angle larger than the critical wave angle into another having a smaller refraction index (sample), the radiation is reflected back into the media with higher density. The critical angle is defined by $\theta_c = \sin^{-1} n_2/n_1$, where n_2/n_1 is the refractive index ratio of the sample to the crystal. A total reflection will occur at $\theta > \theta_c$; the light is partially reflected at $\theta < \theta_c$. These effects are schematically illustrated in Figure 1.

For total reflection, i.e., for $\theta > \theta_c$, the depth of penetration d_p of electromagnetic waves is calculated according to the equation⁸

$$d_p = \frac{\lambda}{2\pi n_1 \left(\sin^2 \theta - \frac{n_2^2}{n_1^2} \right)^{1/2}}$$

where λ is the wavelength, n_1 and n_2 are the refractive indices of the ATR crystal and the sample material, and θ is the angle of incident. In the mid-infrared range the depth of penetration varies from 0.1 μm to approximately 1 μm , depending on the wavelength of the infrared beam, the type

* To whom correspondence should be addressed. E-mail: tuchbr@fmf.uni-freiburg.de.

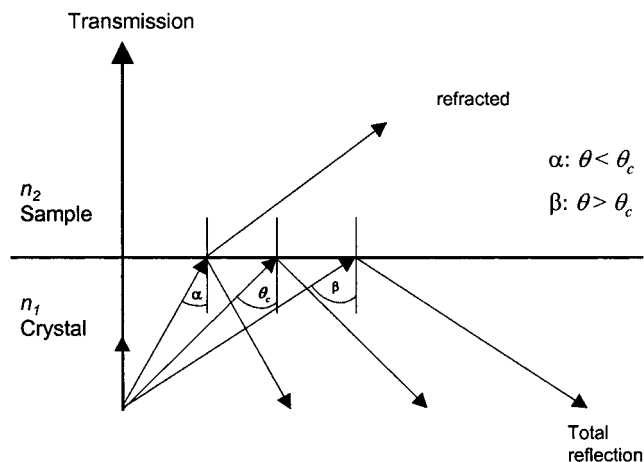


Figure 1. Schematic diagram of the behavior of electromagnetic waves at the interfacial area between phases.

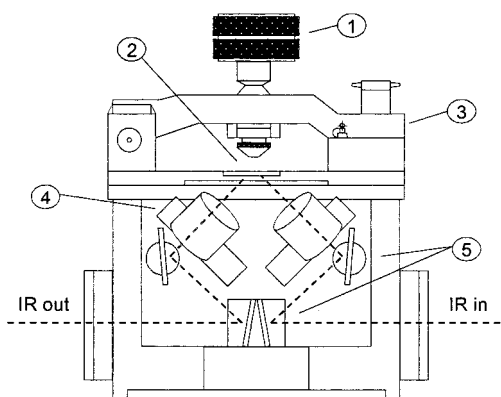


Figure 2. Schematic diagram of side view of the "Golden Gate": (1) torque head screw with limiter screw; (2) ATR crystal area; (3) clamp bridge; (4) lens barrel (ZnSe); (5) mirrors.

of reflection element, and the angle of incidence. Depending on the depth of penetration the penetrating wave is attenuated. The resulting energy loss in the reflected light is referred to as ATR.

All IR spectra were recorded using a "Golden Gate" single-reflection ATR system from LOT-Oriel GmbH & Co. KG. The samples were placed without further preparation on the ATR crystal area and were fixed by a limiter torque head screw that provided a predetermined pressure of 80 lbs to the sample. Every polymer sample was measured three times at different sample points under the same conditions to eliminate the effect of surface inhomogeneities. The schematic diagram of the "Golden Gate" is shown in Figure 2.

Experimental Part

Materials. Dibrom-[2,6-diiso-Ph-DAD(Me,Me)]nickel (DMN) was supplied by Okuda et al. *rac*-Me₂Si(2-Me-4-PhenInd)₂ZrCl₂ (MPI), *rac*-Me₂Si(2-Me-4-NaphInd)₂ZrCl₂ (MNI), *rac*-Me₂Si(2-MeBenzInd)₂ZrCl₂ (*rac*-MBI), *meso*-Me₂Si(2-MeBenzInd)₂ZrCl₂ (*meso*-MBI), *rac*-Me₂Si(Ind)₂ZrCl₂ (I), *rac*-Me₂Si(2-MeInd)₂ZrCl₂ (MI), *rac*-Me₂Si(4,5-BenzInd)₂ZrCl₂ (BI), bis(2-PhenInd)ZrCl₂ (PhInd), bis(2-Me-cyclopenta[1]phenanthryl)ZrCl₂ (MeLig), bis(2-phenylcyclopenta[1]phenanthryl)ZrCl₂ (PhLig), and bis(cyclopenta[1]phenanthryl)ZrCl₂ (HLig) was obtained from BASF AG, 1-hexene and 1-octene from Merck, MAO from Witco

Germany, toluene from Roth GmbH, ethene from Gerling Holz u. Co, Handels-GmbH, Hamburg, and propene from BASF AG. Toluene solvent was refluxed and distilled over Na/K alloy, and 1-hexene and 1-octene were distilled over CaH₂ prior to use. MPI, MNI, *rac*-MBI, *meso*-MBI, I, MI, BI, PhInd, MeLig, PhLig, HLig, ethene, propene, and MAO were used without further purification. All catalyst components, including toluene solvent and monomers, were handled and stored under a dry argon atmosphere. All manipulations of compounds were carried out by standard Schlenk, vacuum, and glovebox techniques.

Polymerization. The copolymerization procedure for ethene/propene and ethene/1-octene has been described previously.⁹ The following catalysts have been used with concentrations given in parentheses: MPI (0.5, 0.75, 1.5 μmol/L), MNI (1 μmol/L), *rac*-MBI (2, 3 μmol/L), *meso*-MBI (3 μmol/L), I (2 μmol/L), MI (2 μmol/L), BI (2 μmol/L), PhInd (10, 20 μmol/L), MeLig (2, 10, 40 μmol/L), PhLig (10, 75 μmol/L), HLig (2, 10, 40 μmol/L). Typically, toluene was used as solvent and MAO as cocatalyst. The reaction pressure was varied between 1 and 2 bar, the reaction temperature was varied between 0 and 60 °C, and the Al/metal molar ratios were varied between 30 000 and 1000 mol (mol⁻¹). The ethene polymerization using DHN is described elsewhere.¹⁰ In accordance with earlier observations by Brookhart and others¹¹ at high polymerization temperatures, low ethene pressure, and methyl substitution of the catalyst, branching of the poly(ethene) is favored, acquiring a polymer structure resembling the structures of ethene/propene polymers.

The copolymerization process of ethene/1-hexene was carried out in an automated 0.6 L high-pressure Parr double-jacket reactor and an external cooling jacket circuit that are connected to fast operating thermostats. Important parameters like reactor temperature, jacket temperature, stirrer rotation speed, and pressure have been controlled and registered by a computer. This reactor system was developed together with Labeq AG in Zürich (Bellariastrasse 33, Switzerland) and Camile Products in BG Philippine (Waterpoortstraat 2/b, The Netherlands). Typically, before the reaction was started, the reactor was automatically flushed and cleaned. Then the reactor was filled with toluene and temperature control was started at a user-defined set point (40 °C). After thermal equilibration was attained, a specified amount of toluenic MAO solution (10%) and a specified amount of 1-hexene were added before the reactor system was flushed with ethene until the reaction mixture was saturated with the monomer gas. The polymerization was started by adding the calculated amount of catalyst MNI (3 μmol/L) or MPI (1 μmol/L) dissolved in 10 mL of toluene. The reaction pressure was kept constant at 2 bar during the polymerization and controlled by a mass flow meter (F-201C-FA, Bronkhorst, NL-7261 AK Ruurlo, The Netherlands). The total volume of the reaction mixture was 300 mL. The formed copolymer was precipitated in 1 L of methanol acidified with 30 mL of 10 wt % aqueous HCl, filtered, and dried at 60 °C under vacuum.

Polymer Characterization. ¹³C NMR spectra were recorded from solutions of 40–60 mg of polymer in 0.5 mL

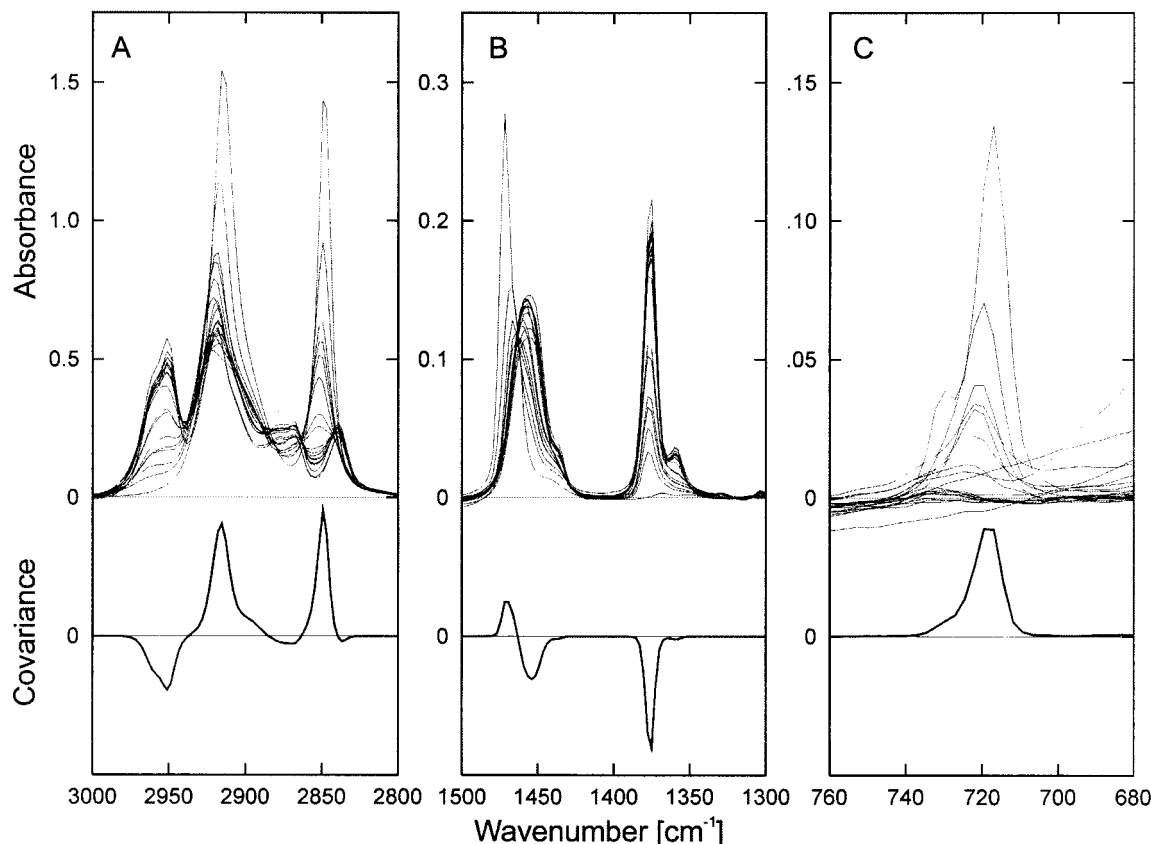


Figure 3. Absorption and covariance spectra of ethene/propene copolymers (data set I) for three different wavenumber ranges.

of $C_2D_2Cl_4$ at 400 K by a Bruker ARX 300 at 75.4 MHz, with a 90° pulse angle, inverse gated decoupling, 5 s delay, and at least 5000 scans. These signals were referenced to $C_2D_2Cl_4$ ($\delta = 74.06$ ppm). The ethene and comonomer incorporation was determined by ^{13}C NMR spectroscopy according to literature procedures.⁴

ATR-FTIR Experiments. A Vektor 22 spectrometer from Bruker combined with a “Golden Gate” single-reflection ATR system was used to record all IR spectra. The FTIR spectrometer was equipped with a deuterated triglycine sulfate (DTGS) detector. Each spectrum was obtained by coadding 20 scans at 4 cm^{-1} resolution using Blackmann–Harris three-term apodization. The “Golden Gate” ATR system consisted of an ATR diamond crystal 45° top plate and beam-condensing lenses made out of ZnSe (see Figure 2).

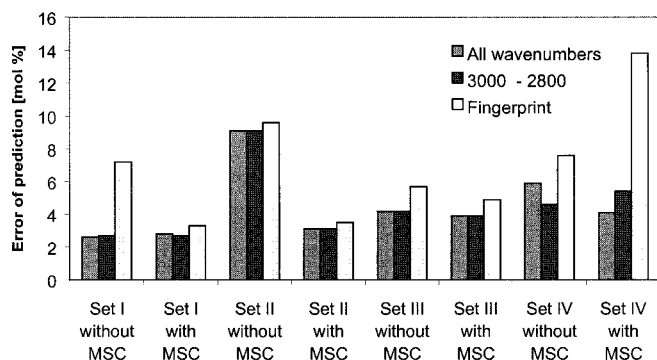
Results and Discussion

IR Spectra. The spectrometer samples the spectrum in the range between 4000 and 600 cm^{-1} with 1784 data points each. Three regions are sensitive to C–H vibrations,¹² namely, $3000\text{--}2800$, $1500\text{--}1300$, and $760\text{--}680\text{ cm}^{-1}$, and are thus suitable for the determination of the comonomer content of copolymers. In Figure 3 the baseline-corrected spectra in these regions are depicted for ethene/propene copolymers. In addition we have plotted the covariance of the absorbance at each wavenumber and the ethene content of the copolymers against the wavenumber.

By use of this covariance spectrum, it is possible to estimate how much information about the composition can

be inferred from each spectral point. As can be seen from Figure 3A the first region ($3000\text{--}2800\text{ cm}^{-1}$) contains three overlapping bands and several shoulders caused by C–H valence vibrations. The covariance spectrum clearly shows that the bands at 2920 and 2850 cm^{-1} are correlated with the ethene content of the copolymers whereas the band at 2950 cm^{-1} and the shoulder at 2880 cm^{-1} are correlated with the propene content. The second region ($1500\text{--}1300\text{ cm}^{-1}$), which is shown in Figure 3B, contains the C–H deformation bands. Near 1460 cm^{-1} , two overlapping bands caused by the CH_2 and CH_3 groups are visible; the symmetric deformation band of the CH_3 group is located at 1380 cm^{-1} . The covariance spectrum shows that the band at 1470 cm^{-1} is caused by the CH_2 groups, whereas the band at 1455 cm^{-1} is due to the CH_3 groups, which is in accordance with the results summarized by Parikh et al.¹³ Finally, the third region ($760\text{--}680\text{ cm}^{-1}$) is dominated by the CH_2 rocking band at 720 cm^{-1} . It is shown in Figure 3C.

Preprocessing. A very important step in obtaining proper analytical standards is the preprocessing of the data, which corrects systematic measurement errors. Especially in the fingerprint region between 1500 and 600 cm^{-1} , strong baseline distortions have been observed¹⁴ that could not be corrected by adjusting instrumental parameters. These distortions are corrected automatically by a modified version of the algorithm proposed by Pearson,¹⁵ which fits a cubic spline with 16 equidistant nodes to the estimated baseline and subtracts it from the spectrum. In addition, multiplicative errors stemming from the different optical, chemical, and



Dataset	Spectral range [cm ⁻¹]	PCR	MSC + PCR
I ethene/propene copolymers	3000-2800, 1500-1300, 760-680	2.6 (4)	2.8 (2)
	3000 - 2800	2.7 (4)	2.7 (2)
	1500 - 1300, 750 - 600	7.2 (3)	3.3 (3)
II ethene/propene copolymers	3000-2800, 1500-1300, 760-680	9.1 (4)	3.1 (2)
	3000 - 2800	9.1 (4)	3.1 (2)
	1500 - 1300, 750 - 600	9.6 (4)	3.5 (4)
III ethene/1-hexene copolymers	3000-2800, 1500-1300, 760-680	4.2 (3)	3.9 (2)
	3000 - 2800	4.2 (3)	3.9 (2)
	1500 - 1300, 750 - 600	5.7 (3)	4.9 (1)
IV ethene/1-octene copolymers	3000-2800, 1500-1300, 760-680	5.9 (4)	4.1 (5)
	3000 - 2800	4.6 (7)	5.4 (4)
	1500 - 1300, 750 - 600	7.6 (7)	13.8 (7)

Figure 4. Optimal standard error of prediction [mol %] and rank (in parentheses) as determined by leave-one-out cross validation for the PCR model with and without MSC.

mechanical properties of the samples are corrected by multiplicative scattering correction (MSC).¹⁶

Determination of Composition. As we have pointed out above, there are two well-separated bands that are sensitive to CH₂ and CH₃ groups, namely, the CH₂ rocking band at 720 cm⁻¹ and the symmetric deformation band of the CH₃ group at 1380 cm⁻¹. However, the band at 720 cm⁻¹ has a poor signal-to-noise ratio, and thus, a direct inference of the composition from these band intensities leads to bad accuracy. Therefore, we used multivariate calibration for the quantitative analysis of the spectra.^{17,18} To establish proper calibration standards, we have formed four data sets from the collected spectra: data set I contains the data of 19 very pure ethene/propene copolymer samples with comonomer incorporations between 0% and 100%. In addition to those samples, data set II also contains the spectra of ethene homopolymers from previous experiments with a similar structure that resembles ethene/propene polymerized samples. These samples also contain unknown impurities that lead to distorted spectra.

Data set III is quite homogeneous. It is built of 18 ethene/1-hexene copolymers synthesized using two different types of catalysts with composition between 0% and 50%. The last set (data set IV) shows the most variability: the 34 ethene/1-octene samples have been synthesized by means of many different catalyst systems and under varied conditions with composition between 0% and 100%.

Multivariate Calibration. For each of the four data sets described above, several multivariate calibration models have been constructed using principle component regression (PCR). Each of the three spectra per sample were used for the estimation of the comonomer content, and the three values were averaged. To find the best calibration, we have

varied the preprocessing of the data (with or without MSC) and combined different wavenumber regions. The error of each calibration model was estimated by leave-one-out cross validation, which was also used to find the optimal number of principal components to keep (the so-called rank). Note that all optimal ranks satisfy the condition $k \leq m/4$, where k is the rank and m the number of samples in the calibration set. This condition ensures that the data are not overfitted.

Discussion of the Results. As can be seen from Figure 4, the error of prediction for short branches is in general lower than for longer branches. For ethene/propene copolymers the error is about 3%, for ethene/1-hexene we find 4%, and for ethene/1-octene the error is approximately 5%. This is due to the fact that the IR spectra as well as the ¹³C NMR spectra are most sensitive to the ratio of CH and CH₃ to CH₂ groups, which in turn depends on the composition of the copolymer. Because shorter side branches lead to a larger ratio than longer side branches, the performance of the calibration is better for short branches.

The preprocessing of the data also has a significant influence on the quality of the calibration. For most cases, the same or a better accuracy of the calibration can be obtained with fewer factors for the MSC-corrected data. Thus, multiplicative effects play an important role in our study. These effects are particularly pronounced for data set II, where samples with moderate interferent concentrations are contained. Here, the multiplicative effects cannot be corrected by including more factors in a purely linear approach; even with four factors the performance of the calibration is very poor without MSC.

Finally, we have also found that the bands in the spectral region between 3000 and 2800 cm⁻¹ are more suited for a calibration than the bands in the fingerprint region. Although

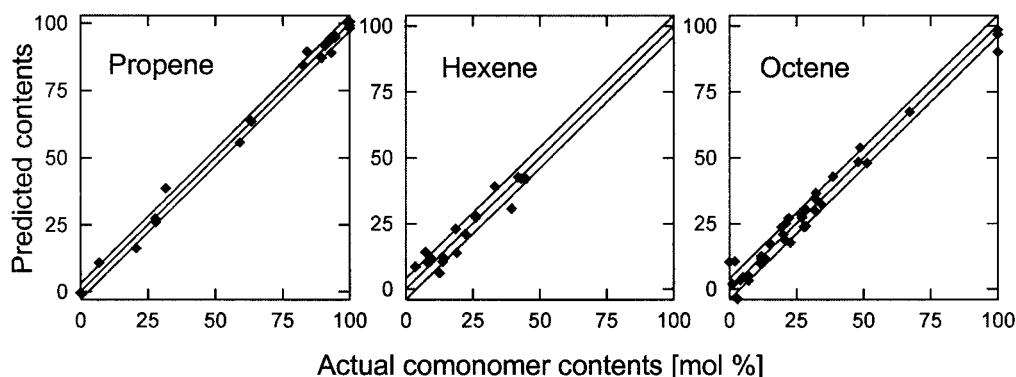


Figure 5. Predicted vs actual comonomer content (as determined by ^{13}C NMR spectroscopy) for ethene/propene, ethene/1-hexene, and ethene/1-octene copolymers. The lines indicate the 1σ intervals.

the bands in this region have a strong overlap, which would make a direct computation of band intensities hardly feasible, the better signal-to-noise ratio in this region leads to a higher sensitivity of the multivariate calibration.

To visualize the performance of the calibration, we have depicted in Figure 5 the predicted values against the true values for the comonomer incorporation for the best calibrations obtained for data sets II, III, and IV.

It is important to note that in general the quality and usefulness of an analytical method, which is *exclusively* based on statistical inference, crucially depend on the proper choice of calibration standards. All variations, which are expected to be observed in the samples, must be taken into account for the choice of the calibration standards. Otherwise, the values obtained by applying the calibration method might not be reliable. Thus, strictly speaking, the results presented here should be valid only for olefin copolymers, which are produced using metallocene catalysts of the types described above.

However, by choosing appropriate spectral regions, the calibration methods presented in this article explicitly make use of prior spectroscopic knowledge and thus do not rely on statistics alone. The prediction of the composition is based on the ratio of CH and CH_3 to CH_2 groups, and therefore, we expect the calibration methods to yield reliable values for olefin copolymers and ethene homopolymers with methyl side groups resembling ethene/propene polymers. Moreover, we emphasize that IR spectroscopy is mostly sensitive to small substructure groups. Hence, we do not expect that these methods can distinguish between a real copolymer and blends of homopolymers.

Conclusion

In summary, we have demonstrated that ATR-FTIR spectroscopy together with the "Golden Gate" single-reflection ATR system provides a very efficient and reliable spectroscopic technique for fast polymer analysis. The data acquisition is significantly speeded up in comparison to ^{13}C NMR spectroscopy where the typical average measurement time is about 5 h at 5000 scans per sample. Compared to conventional FTIR spectroscopy, where additional sample preparation time is needed, the throughput of samples can be increased from 2 probes per hour to 40 per hour by utilizing ATR-FTIR spectroscopy. This high-throughput rate

is necessary for analyzing copolymer samples produced by novel catalyst systems synthesized in screening experiments using our fully automated robotic system provided by Chemspeed, Ltd. in Augst (Switzerland). The quality of the spectroscopic data is sufficient to establish proper calibration standards using multivariate calibration techniques, and error estimates have been obtained using cross validation.

Acknowledgment. The authors thank the Bundesministerium für Bildung und Forschung and BASF AG for funding of this project (Förderkennzeichen 03N8012) and M. O. Kristen and D. Lilge from BASF AG for helpful discussions on this material.

References and Notes

- (1) Jandeleit, B.; Schaefer, D. J.; Powers, T. S.; Turner, H. W.; Weinberg, W. H. *Angew. Chem.* **1999**, *111*, 2648–2689.
- (2) Weinmann, H. *Nachr. Chem.* **2001**, *49*, 150–154.
- (3) Tuchbreiter, A.; Mülhaupt, R. *Macromol. Symp.* **2001**, *173*, 1–20.
- (4) Randall, J. C. *J. Macromol. Sci., Rev. Macromol. Chem. Phys.* **1989**, *C29* (2–3), 201–317.
- (5) Blitz, J. P.; McFaddin, D. C. *J. Appl. Polym. Sci.* **1994**, *51*, 13–20.
- (6) Harrick, N. J. *J. Phys. Chem.* **1960**, *64*, 1110–1114.
- (7) Fahrenfort, J. *Spectrochim. Acta* **1961**, *17*, 698–709.
- (8) Harrick, N. J. *Internal Reflection Spectroscopy*; Wiley: New York, 1967.
- (9) (a) Jüngling, S.; Kotzenburg, S.; Mülhaupt, R. *J. Polym. Sci., Part A* **1997**, *35*, 1–8. (b) Schneider, M. J.; Suhm, J.; Mülhaupt, R.; Prosenic, M.-H.; Brintzinger, H.-H. *Macromolecules* **1997**, *30*, 3164–3168. (c) Schneider, M.; Mülhaupt, R. *J. Mol. Catal. A: Chem.* **1995**, *101*, 11–16. (d) Suhm, J.; Schneider, M. J.; Mülhaupt, R. *J. Polym. Sci., Part A* **1997**, *35*, 735–740.
- (10) Suhm, J.; Heinemann, J.; Thomann, Y.; Thomann, R.; Maier, R.-D.; Schleis, T.; Okuda, J.; Kressler, J.; Mülhaupt, R. *J. Mater. Chem.* **1998**, *8* (3), 553–563.
- (11) (a) Johnson, L. K.; Killian, C. M.; Brookhart, M. *J. Am. Chem. Soc.* **1995**, *117*, 6414–6415. (b) van Koten, G.; Vrieze, K. *Adv. Organomet. Chem.* **1982**, *21*, 151–239.
- (12) Hesse, M.; Meier, H.; Zeeh, B. *Spektroskopische Methoden in der organischen Chemie* (Spectroscopic Methods in Organic Chemistry); Georg Thieme Verlag: Stuttgart, New York, 1995.
- (13) Parikh, A. N.; Gillmor, S. D.; Beers, J. D.; Beardmore, K. D.; Cutts, R. W.; Swanson, B. I. *J. Phys. Chem. B* **1999**, *103*, 2850–2861.
- (14) Saloma, I. K.; Kauppinen, J. K. *Appl. Spectrosc.* **1998**, *52*, 579–586.
- (15) Pearson, G. A. *J. Magn. Reson.* **1977**, *27*, 265–272.

- (16) Geladi, P.; MacDougall, D.; Martens, H. *Appl. Spectrosc.* **1985**, 39, 491–500.
- (17) Martens, H.; Næs, T. *Multivariate Calibration*; Wiley: Chichester, U.K., 1991.

- (18) Otto, M. *Chemometrie (Chemometrics)*; VHC: Weinheim, Germany, 1997.

CC010033Q